Native oxide and ion implantation damaged layers on silicon carbide studied by ion beam analysis and ellipsometry

Z. Zolnai[a], N. Q. Khánh[a], E. Szilágyi[b], Z. E. Horváth[a] and T. Lohner[a]

[a] *Research Institute for Technical Physics and Materials Science, H-1525 Budapest, P.O.B. 49 Hungary*
[b] *Research Institute for Particle and Nuclear Physics, H-1525 Budapest, P.O.B. 49 Hungary*

Abstract

Thickness of the native oxide layer formed on chemically cleaned 4H-SiC was measured by $^{16}O(\alpha,\alpha)^{16}O$ resonance method and ellipsometry and found to be 0.7 nm and 1.3 nm, respectively. The knowledge of the magnitude of the native oxide is important to construct optical model for ion implanted SiC. Damage distribution created by Al^+ ions was characterized by Backscattering Spectrometry in combination with channeling (BS/C), ellipsometry and cross-sectional transmission electron microscopy (XTEM) methods. Al^+ ions with energy of 200 keV were implanted at room temperature into SiC and Si samples to create disorder. According to BS/C considerably larger damage was found in SiC than in Si. The damage distribution determined by different methods will be discussed.

Keywords: native oxide, silicon carbide, ion implantation, Backscattering Spectrometry, channeling, transmission electron microscopy, ellipsometry

I. Introduction

Silicon carbide is a wide bandgap semiconductor with high thermal conductivity, high saturation velocity of carriers, high critical electric breakdown field and radiation resistance. Due to the unique combination of these properties, SiC is a promising candidate for the fabrication of devices operating under extreme conditions, such as high temperature, high power, high frequency and high radiation levels [1-3].

The processing of SiC is complicated because of the high temperatures (>1800 ^{o}C) necessary for dopant diffusion. An alternative method to selectively dope defined regions of SiC is ion implantation. Implantation process is not constrained by thermodynamic limitations and allows species of very low diffusivities to be easily introduced. However, ion beam irradiation damages the crystal lattice of SiC [4-12], many aspects of the damaging process have not completely clarified. Aluminum has received a great deal of attention as acceptor in SiC due to its low activation energy (0.24 eV).

In this paper the damage in aluminum implanted 4H-SiC was studied by ion beam analitical methods, ellipsometry and cross-sectional transmission electron microscopy. SiC is the only compound semiconductor whose native oxide is silicon oxide. To construct an appropriate optical model of ion implanted SiC for ellipsometry, the knowledge of the magnitude of native oxide is important. Native oxide thickness for ion implanted 4H-SiC was extracted also from ellipsometric measurement.

II. Experimental

Single crystal 4H-SiC samples (from CREE Res. Inc.) and Si samples were cleaned by chemical treatment.

These samples were implanted with 200 keV Al^+ ions at room temperature. The implanted fluence was $8x10^{13}/cm^2$. To amorphize the near surface region after Al implantation one 4H-SiC sample was irradiated with 200 keV Xe^+ ions at room temperature using a fluence of $3x10^{13}$ Xe^+/cm^2.

Ion beam studies were performed in a scattering chamber with a two-axis goniometer connected to a 5 MV Van de Graaff accelerator. He^+ beam was collimated with two sets of four-sector slits to the dimensions of 0.5×0.5 mm^2, while the beam divergence was kept below 0.04 deg. In the experimental chamber the vacuum was better than 1×10^{-4} Pa using liquid N_2 cooled traps along the beam path and around the wall of the scattering chamber. Backscattered He^+ ions were detected using an ORTEC surface barrier detector mounted in Cornell geometry. To reduce the damage created by the beam itself [13,14] low current of 3 nA was used during the measurements and monitored by a transmission Faraday cup [15]. BS spectra were evaulated using RBX code [16].

The thickness of nativ oxide was determined via resonance measurements with the 10 keV wide $^{16}O(\alpha,\alpha)^{16}O$ resonance at 3045 keV [17]. The maximum of the cross section for oxygen at detection angle of 165° is higher by a factor of 17 than the Rutherford cross section value.

To investigate the damage caused by ion implantation BS/C measurements were performed with 3500 keV He^+ beam. In this case, to increase the depth resolution at the surface a glancing detection angle of 97° was used [18].

Cross sectional specimen for transmission electron microscopy was prepared by ion beam milling. The specimen was investigated in a Philips CM20 electron microscope (TWIN configuration).

In order to determine the index of refraction and the extinction coefficient of the samples, multiple angle of incidence ellipsometry measurements were performed using a manual null ellipsometer at wavelength of 632.8 nm (He-Ne laser).

III. Results and discussion

To determine the amount of oxygen atoms in the native oxide layer on unimplanted pure 4H-SiC and for comparison, on Si, excitation curves of $^{16}O(\alpha,\alpha)^{16}O$ were measured in the energy range of 3030-3060 keV. To reduce the background the samples were aligned. A typical 165° aligned BS spectrum of SiC at the resonance energy is demonstrated in Fig. 1 together with the energy window for counts integration. The excitation curves, i. e., integrated counts of oxygen peak in the BS spectra after substraction of background versus incident energy of $^4He^+$ ions are shown in Fig. 2. RBX simulated excitation curves of SiO_2 layers with several thicknesses are also shown. Assuming that oxygen signal arises just from the native oxide and the native oxide is a stoichiometric silicon dioxide film we can deduce an equivalent layer thickness. SiO_2 thicknesses were extracted from measured data and simulated curves by minimizing the sum of the squares of the deviation of the simulated curve from the experimental points in the energy range of 3040-3050 keV. Using $6.67x10^{22}$ $atom/cm^3$ as density of SiO_2 the calculated SiO_2 thicknesses are 0.7 nm for 4H-SiC and 0.8 nm for Si, respectively.

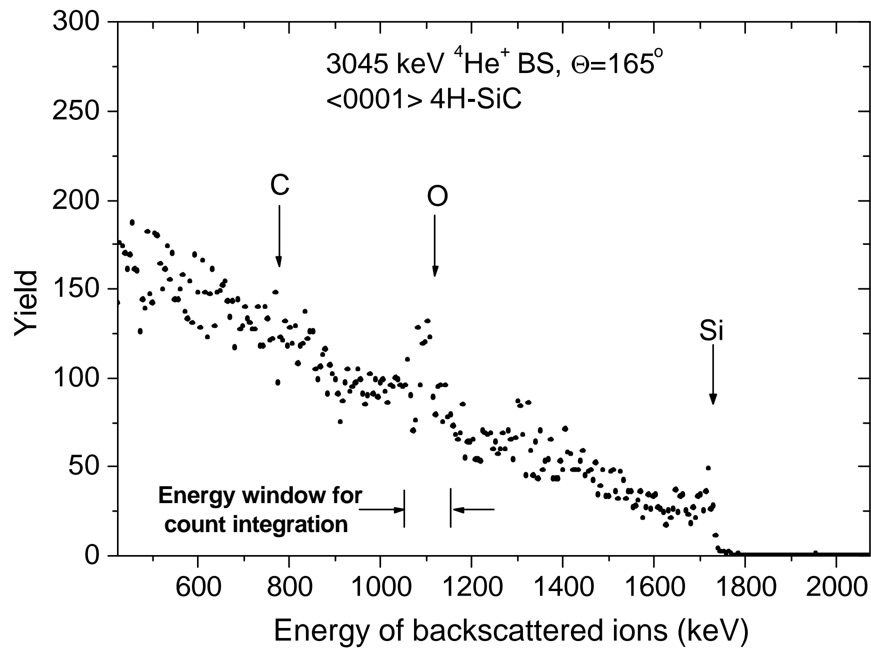

Fig. 1 *<0001> aligned BS spectrum of 4H-SiC sample using nuclear resonance peak at 3045 keV in the cross section of* $^{16}O(\alpha,\alpha)^{16}O$ *reaction. The energy window for counts integration is also shown.*

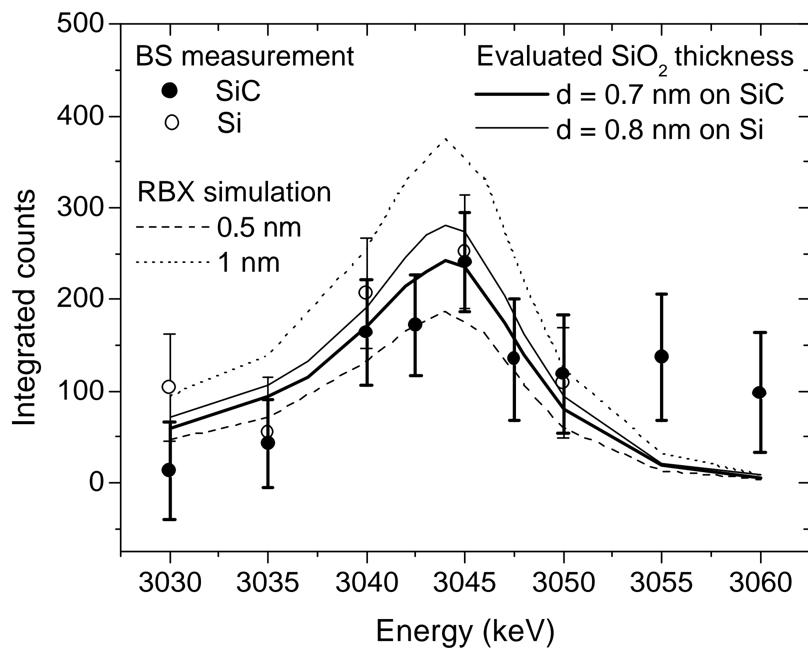

Fig. 2 *Measured excitation curves for unimplanted <0001> 4H-SiC and <100> Si and simulated excitation curves for thin silicon dioxide layers with several thicknesses. The extracted* SiO_2 *thicknesses are also shown.*

The thickness of native oxide on the unimplanted SiC sample was also investigated by ellipsometry. In Fig. 3 measured and calculated ellipsometric angles as a function of the angle of incidence for 4H-SiC sample are shown. To obtain the oxide thickness a simple one layer model was used (i.e. a surface layer on bulk SiC). The layer thickness, the refractive index and the extinction coefficient for this surface layer was determined. The thickness of the surface layer, which is most probably the native oxide layer is obtained as 1.3 nm. This value is greater than that of determined by the resonance method. The time interval between cleaning of the samples and the measurement in the case of BS/C was six days, while in the case of ellipsometry was seven days, so the difference between the two results can hardly originate from this condition. However, a possible surface roughness of the sample can contribute to the thickness of the surface layer in the case of ellipsometry while the effect of surface roughness can be neglected in BS measurement.

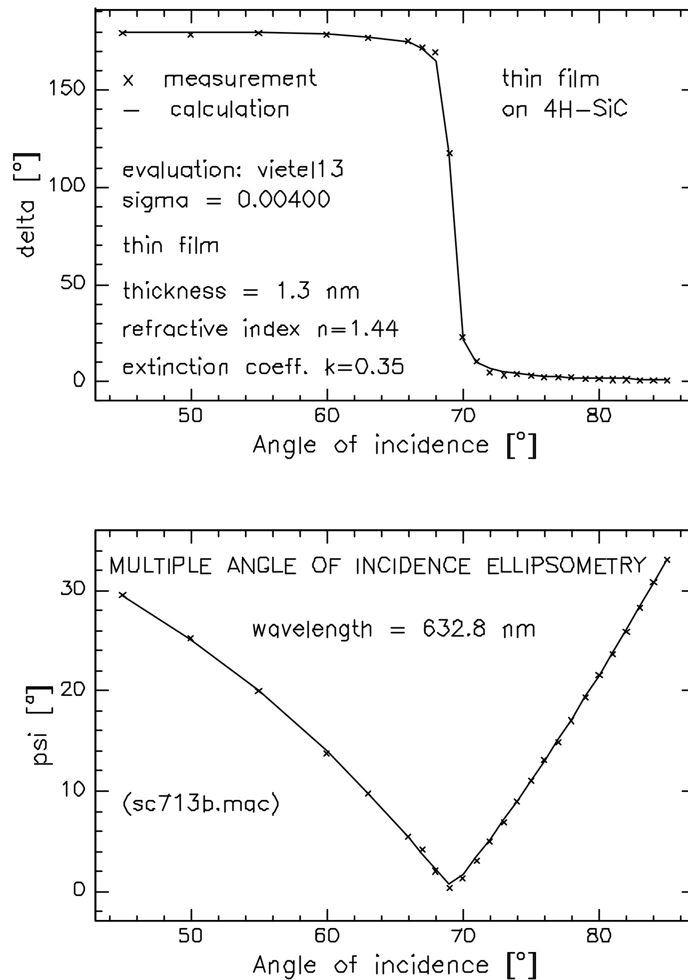

Fig. 3 *The measured and calculated ellipsometric angles in function of the angle of incidence for 4H-SiC sample. Evaluated native oxide layer thickness is also shown.*

The damage distributions created by Al implantation into SiC and Si samples were investigated by BS/C and XTEM. Fig. 4 shows 97° BS channelled and random spectra of 200 keV, $8x10^{13}$ Al^{+}/cm^{2} implanted 4H-SiC at room temperature together with the cross-sectional TEM micrograph of the same sample. In the BS spectra the broad peak behind the Si edge where the implanted aligned BS spectrum reaches the random level indicate a buried disorder. A slightly damaged region near the surface can be observed.

The same feature can be observed in XTEM micrograph in Fig. 4. There is a single-crystalline sublayer of about 30 nm thickness at the sample surface, followed by an about 60 nm thick partially amorphized layer. Underneath a 200 nm thick buried amorphous layer was formed. The next zone is partially damaged which is followed by the undamaged single-crystalline bulk material. Results of BS measurements and TEM observation are comparable throughout the same depth scale shown in Fig. 4. There is a good agreement between results of the two independent methods considering the slightly damaged near surface region and the buried amorphous zone.

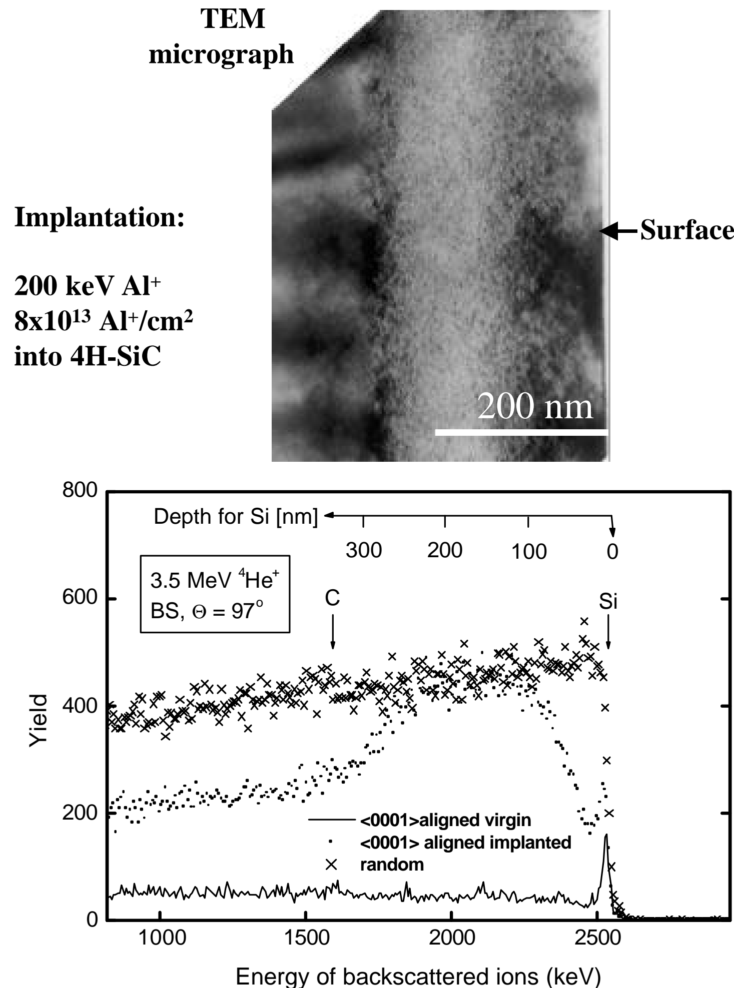

Fig. 4 *97° Backscattering spectra and cross-sectional TEM micrograph of Al^+ implanted 4H-SiC sample. Aligned BS spectra were measured along the <0001> axis. Depth scales for comparison are also shown.*

Fig. 5 shows 97° BS spectra of 200 keV, $8x10^{13}$ Al^+/cm^2 implanted Si at room temperature. Ion irradiation under the same experimental conditions produced considerably less damage in silicon than in 4H-SiC. The reason can be the difference in the dynamic defect annealing for SiC and Si during the ion bombardment. In connection with this, considerations on the effect of local temperature on primary defect production are essential [19].

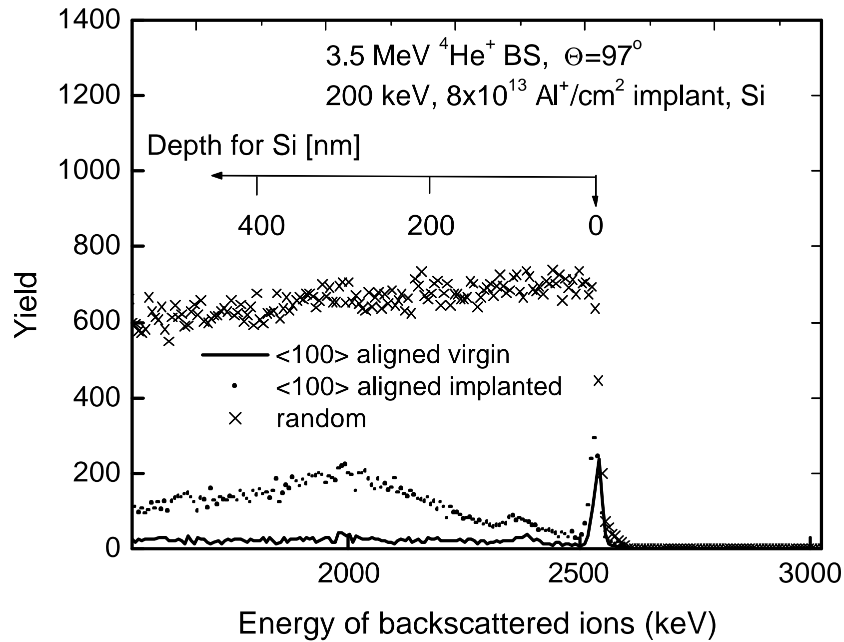

Fig. 5 *97° Backscattering spectra of Al^+ implanted Si sample. Aligned spectra were measured along the <100> axis.*

A 200 keV, 8x10^{13} Al^+/cm^2 implanted 4H-SiC sample post implanted with 200 keV, 3x10^{13} Xe^+/cm^2 was investigated by multiple angle of incidence ellipsometry. The double implantation created a completely amorphized near surface region. A two layer model was used (native oxide layer assumed as SiO_2, amorphous SiC layer and single crystalline SiC substrate). The refractive index, the extinction coefficient, and the thickness of completely amorphized SiC and thickness of the native oxide layer were extracted from measured data. The refractive index and extinction coefficient of the crystalline SiC were taken from the literature as reference data [20]. The thickness obtained of completely amorphized layer was found to be 254 nm which agrees well with that extracted from BS measurement (See in Fig. 4 the edge of the buried disorder on the bulk side in BS spectrum which did not change after Xe implantation). Evaluated refractive index and extinction coefficient of completely amorphized SiC are 3.01 and 0.53, respectively.

The thickness value of 2.5 nm extracted for the native oxide layer is somewhat higher than that was found for the unimplanted case. The reason of it may be the influence of implantation on the oxidation behavior of SiC.

IV. Conclusion

Thickness of the native oxide layer was measured on chemically cleaned pure 4H-SiC by $^{16}O(\alpha,\alpha)^{16}O$ resonance method and ellipsometry and on 200 keV Al and 200 keV Xe implanted 4H-SiC by ellipsometry. The thickness of the native oxide layer was found to be thicker for the fully amorphized SiC than that was found for the unimplanted one.

The thickness of the buried disorder created by implanted Al^+ ions into 4H-SiC was characterized using BS in combination with channeling and XTEM. The two independent methods with reasonable agreement showed a 200 nm thick completely amorphized layer in SiC. Considerable less damage was observed in silicon than in 4H-SiC in the case of ion irradiation under the same implantation conditions.

Acknowledgments

Partial support from Hungarian Science Research Foundation (OTKA grant No. T030441, No. T025928 and No. T032029) is greatly appreciated. This work was partially funded by Foundation for Students of Technical University of Budapest. The authors would like to thank P. Deák for supplying them 4H-SiC substrate and J. Waizinger for performing ion implantation.

References

[1] G.L. Harris, editor, Properties of Silicon Carbide, EMIS Datareviews Series No. 13, 1995
[2] C.I. Harris, A. O. Konstantinov, Physica Scripta, T79 (1999) pp 27-31.
[3] J. A. Jr.Cooper, Phys. Stat. Sol. (a) 162 (1997) pp. 305-320.
[4] M. G. Grimaldi, L. Calcagno, P. Musumeci, N. Frangis, Van Landuyt, J.J. Appl. Phys. 81 (1997) pp. 7181-7185
[5] M.V.Rao, P. Griffith, O. W. Holland, G. Kelner, J.A.Jr.Freitas, D. S. Simons, P.H.Chi, J. Appl. Phys. 77 (1995) 2479-2485
[6] T. Troffer, M. Schadt, T. Frank, H. Itoh, G. Pensl, J. Heindl, H. P. Strunk, M. Maier, Phys Stat Sol(a), 162 (1997) pp. 277-298
[7] W. Jiang, W. J. Weber, S. Thevuthasan, D. E. McCready, Nuclear Instruments and Methods In Physics Research B 148 (1999), pp. 557-561
[8] M. Satoh, K. Okamoto, Y. Nakaike, K. Kuriyama, M. Kanaya, N. Ohtani, Nuclear Instruments and Methods In Physics Research B 148 (1999), pp. 567-572.
[9] A. Hallén, A. Henry, P. Pallegrino, B. G. Svensson, D. Aberg, Materials science and Engineering B, 61-62 (1999) 562-566.
[10] W. Jiang, W. J. Weber, S. Thevuthasan, D. E. McCready, Nuclear Instruments and Methods in Physics Research B 148 (1999), pp. 562-566.
[11] A. Heft, E. Wendler, J. Heindl, T. Bachmann, E. Glaser, H. P. Strunk, W. Wesch, Nuclear Instruments and Methods in Physics Research B 113 (1996), pp. 239-243.
[12] E. Valcheva, Paskova, I. G. Ivanov, R. Yakimova, Q. Wahab, S. Savage, N. Nordell, C. I. Harris, Journal of Vacuum Science and Technology B: Microelectronics and Nanometer Sctructures 17 (1999) 1040-1044.
[13] N. Q. Khánh, Z. Zolnai, T. Lohner, L. Tóth, L. Dobos, J. Gyulai, Nuclear Instruments and Methods in Physics Research B 161-163 (2000) pp. 424-428
[14] W. Fukarek, R. A. Yankov, W. Anward, V. Heera, Nuclear Instruments and Methods in Physics Research B 142 (1998) pp. 561-570
[15] F. Pászti, A. Manuaba, C. Hajdu, A. A. Melo and M. F. Da Silva, Nuclear Instruments and Methods in Physics Research B 47 (1990), pp. 187-192
[16] E. Kótai, Nuclear Instruments and Methods In Physics Research B 85 (1994), pp. 588-596.
[17] G. Mezey, E. Kótai, P. Révész, A. Manuaba, T. Lohner, J. gyulai, M. Fried, Gy. Vizkelethy, F. Pászti, G. Battistig and M. Somogyi, Acta Physica Hungarica 58 (1-2), (1985) pp. 39-55
[18] E. Szilágyi, Nuclear Instruments and Methods In Physics Research B 161-163 (2000), pp. 2037-2047.
[19] J.Gyulai, F. Pászti, E. Szilágyi, Nuclear Instruments and Methods In Physics Research B 106 (1995), pp. 328-332.
[20] Choyke W.J., Palik E.D., in Handbook of Optical Constants, edited by Palik E.D.